OPTIMIZATION OF FACET OPTICS*

M-H. Wang[#], F-J. Decker, N. Lipkowitz, Y. Nosochkov, G. White, U. Wienands,
M. Woodley, G. Yocky, SLAC, Menlo Park, CA 94025, USA

Abstract

The FACET accelerator facility is designed to provide short and intense e- or e+ bunches with small spot size for plasma wakefield accelerator research and other experiments. It is based on the SLAC linac with a compressor chicane in sector-10, and a second compressor chicane and final focus in sector-20 (S20). Originally, the S20 chicane was designed to be compatible with an upgrade to include a second S20 chicane for simultaneous transport of e- and e+ bunches. This placed additional optics constraints which led to strong focusing in the S20 chicane. This increased the effects of errors, causing emittance growth. Lately, it has been decided not to proceed with the upgrade option. Therefore, there is the potential for improving the optics by relaxing the constraints. In this study, we explore alternative optics designs where β functions in the S20 chicane and final focus are reduced in order to minimize the error effects. The optics and non-linear aberrations are evaluated, and the chromatic correction is optimized for each design. Beam tracking simulations are performed using elegant[1]. The most optimal designs are identified based on these simulations.

INTRODUCTION

The original FACET design has peak β_x/ β_y values of 900/400 m in the S20 chicane and peak β_x value of 1600 m in the Final Focus region (FF). In this paper we investigate new options for the FACET lattice with reduced maximum β functions in the FF and the chicane. The lower β_x in the chicane will also help to reduce the beam loss in the second chicane dipole where the physical aperture is small. The high β_x in the FF is due to insufficient strength of QFF6, the last FF quadrupole, at beam energy of 23 GeV. Since FACET is presently operating at lower energy of 20.35 GeV, the QFF6 focusing strength can be increased resulting in peak β_x in the final focus reducing from 1600 m to 400 m. The lower β functions in the FF and chicane reduce the natural chromaticity and sensitivity to magnet errors and non-linear effects. However the sextupole strengths to correct the chromatic effect may increase due to the lower β function. The performance of these lattice designs need to be investigated.

A total of six cases including the original FACET lattice (case 1) are studied. The peak β values in chicane, peak β values in FF and β*x/ β*y at IP of these cases are listed in Table 1. The optics functions for these cases are shown in Fig. 1.

Table 1: Summary of peak β values and β* at IP for different FACET designs

unit: m	chicane $\beta_{x,max}$	$\beta_{y,max}$	FF $\beta_{x,max}$	$\beta_{y,max}$	IP $\beta*_x$	$\beta*_y$
Case 1	900	400	1600	250	0.018	0.18
Case 2	900	400	400	300	0.018	0.18
Case 3	400	200	400	300	0.018	0.18
Case 4	150	150	130	100	0.054	0.54
Case 5	150	150	110	60	0.1	1.0
Case 6	150	150	30	60	0.5	5.0
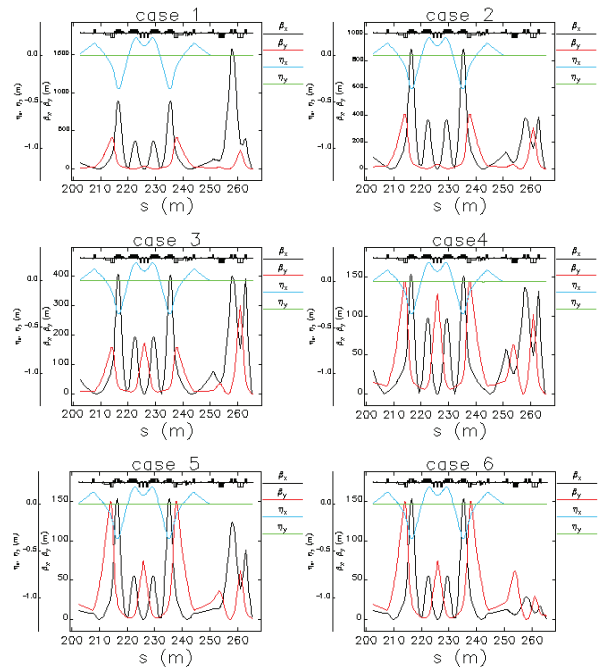
Figure 1: Optics functions in different FACET designs.

CHROMATIC EFFECTS

The FACET beam is highly compressed. The energy spread of the electron bunch can be as large as 1.2×10^{-2} at bunch charge of 3.2 nC. The non-linear chromatic aberrations could blow up the beam distribution at the IP significantly. The chromatic effects need to be minimized when designing the optics. In Table 2, we first list the chromatic terms without sextupoles, where WX, WY are chromatic amplitude functions obtained in MAD calculation [2]. DDX and DDPX are second order dispersion and its derivative, respectively. $T_{j,k,l}$ are the terms in the FACET second order transfer matrix calculated by MAD. The values of WX and WY decrease from case 1 to case 4 as peak β functions decrease. The

amplitude of second order dispersion increases as β functions decrease.

Table 2: Chromatic Terms at IP with Sextupole Off

	Case 1	Case 2	Case 3	Case 4	Case 5	Case 6
WX	2092	1776	983	390	274	236
WY	232	272	94	44	88	79
DDX	0.00	-0.01	-0.01	-0.04	-0.16	-0.61
DDPX	-2.64	-2.63	-3.58	-2.69	-2.66	-0.65
T116	-18.24	-15.40	-12.88	-12.65	-13.65	-14.25
T126	-48.00	-40.21	-36.07	-31.11	-38.77	-40.60
T336	18.33	20.76	10.94	6.77	20.36	33.49
T346	-58.74	-63.91	-39.83	-77.91	221.38	276.92
T566	-0.30	-0.30	-0.30	-0.30	-0.30	-0.30

In order to evaluate how these terms affect the beam distribution at IP, we define σ_{ratio} as:

$$\sigma_{ratio} = \frac{\sigma_j}{\sigma_{j,0}} = \sqrt{1 + \frac{\sum\limits_{k,l} T_{j,k,l}^2 \sigma_{k,ini}^2 \sigma_{l,ini}^2}{\sigma_{j,0}^2}} \qquad (1)$$

Where $\sigma_{j,0}$ is the ideal j-th standard deviation of beam distribution at the IP, $\sigma_{k,ini}$ and $\sigma_{l,ini}$ are the k-th and l-th beam sizes at the beginning of FACET. A scan of $\sigma_{x,ratio}$ and $\sigma_{y,ratio}$ versus energy spread with sextupole off is shown in Fig.2.
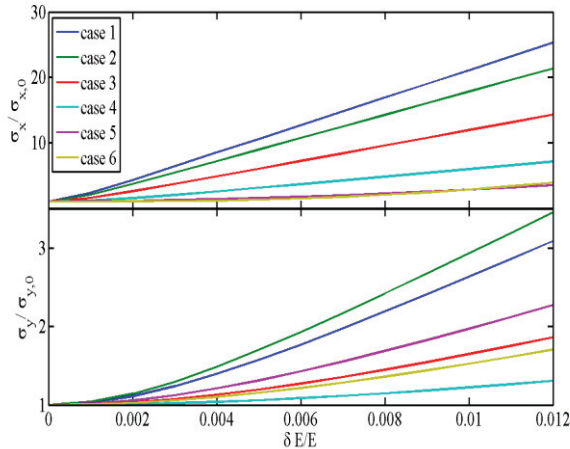
Figure 2: $\sigma_{x,ratio}$ and $\sigma_{y,ratio}$ versus energy spread with sextupoles off. The lower β function lattices reduce chromatic effects and beam size growth.

One can see that the lower β function lattices reduce chromatic effects compared to high β function lattices. The growth of $\sigma_{x,ratio}$ and $\sigma_{y,ratio}$ shown in Fig. 2 is consistent with the trend of WX and WY listed in Table 2. Case 6 has the smallest $\sigma_{x,ratio}$ and case 4 has the smallest $\sigma_{y,ratio}$ as shown in Fig. 2. The term $\sigma_{k,ini}*\sigma_{l,ini}$ in Eq. (1) is

shown in Fig. 3. It acts as a weighting factor to the non-linear aberrations effect. The smaller value of $\sigma_{k,ini}*\sigma_{l,ini}$ helps reducing the beam growth, however the complete effect also depends on the T-term.
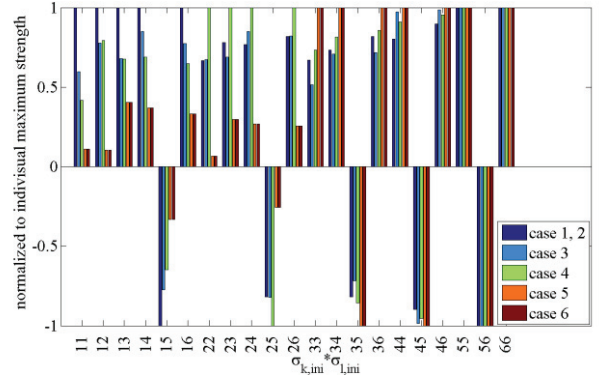
Figure 3: $\sigma_{k,ini}*\sigma_{l,ini}$ is a weighting factor to the non-linear aberrations effect (normalized to the maximum value of individual term).

CHROMATIC CORRECTION

A set of three sextupole families in the S20 chicane is used to correct the chromatic effects. The sextupole strengths are displayed in Fig. 4. They were obtained in a MAD minimization of WX, WY, DDX and DDPX. No correlation was found between sextupole strength and peak β function in the chicane. Intuitively, higher sextupole strength is needed when the β function at the sextupole is small. However it also depends on chromaticity. The chromatic terms with the sextupole correction are shown in Table 3.

Table 3: Chromatic Terms with Sextupole Correction

	Case 1	Case 2	Case 3	Case 4	Case 5	Case 6
WX	66	54	73	40	64	23
WY	122	155	68	25	43	32
DDX	0.00	0.00	0.00	0.00	-0.02	-0.16
DDPX	-0.12	-0.46	-0.24	0.31	-0.38	-0.17
T116	-2.47	-2.08	-2.81	-3.39	-0.45	-0.39
T126	-23.44	-19.44	-20.45	-16.62	-15.94	-12.20
T336	9.10	10.56	10.90	4.86	7.11	4.69
T346	-33.25	-36.08	-42.35	-72.78	97.88	67.75
T566	-0.09	-0.12	-0.10	-0.06	-0.11	-0.14

Similar energy spread scans with sextupoles turned on are shown in Fig. 5. The chromatic aberrations are corrected compared to Fig. 2. However, the sextupoles geometric terms enlarge the bunch distribution. This can be observed when the energy spread is zero in Fig. 5. The $\sigma_{x,ratio}$ and $\sigma_{y,ratio}$ do not go to 1 as compared to Fig. 2.
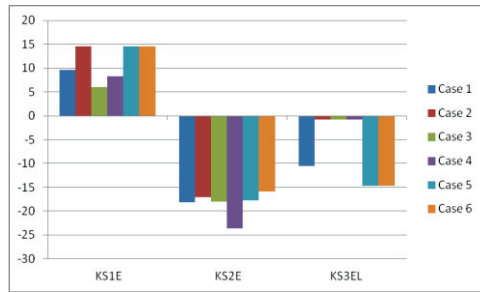
Figure 4: Sextupole strength optimized in MAD.
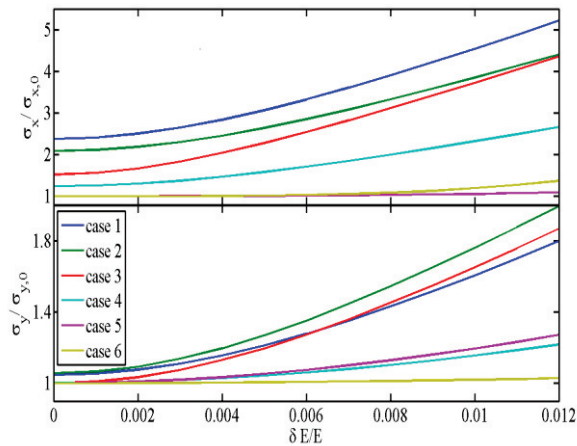
Figure 5: $\sigma_{x,ratio}$ and $\sigma_{y,ratio}$ versus energy spread with sextupoles on. Note that $\sigma_{x,ratio}$ and $\sigma_{y,ratio}$ are not equal to 1 when energy spread is zero. This indicates the geometric contributions from sextupoles.

We also use elegant [1] to include the effects of non-linear aberrations, coherent and incoherent synchrotron radiation on the beam distribution. The initial bunch distribution contains 100,000 particles with total charge of 3.2 nC at beam energy of 20.35GeV. The normalized x-emittance is 50 μm.rad and normalized y-emittance is 5 μm.rad. Two different initial bunch distributions are used in simulation. The first one is a realistic full compression bunch from the linac with energy spread of 1.2×10^{-2} and bunch length of 52 μm. The other is with the same transverse distribution and bunch length but without energy spread. These two bunch distributions are used to investigate the effect of energy spread. The effect of synchrotron radiation is also studied by turning the CSR/ISR effect on/off in elegant simulation. The final distribution at the main IP is analyzed using both Gaussian fitting and standard rms fitting of the bunch distribution. The Gaussian fitting gives the core bunch size while the standard rms deviation reflects the tail. A summary of Gaussian fitting beam sizes at the main IP is shown in Table 4. The standard deviations of the bunch distributions are summarized in Table 5.

Table 4: Gaussian Beam Size at the Main IP

Gaussian beam size	CSR/ISR off w/o dp/p		CSR/ISR off, with dp/p		CSR/ISR on, with dp/p		Relative growth of Gaussian beam size	
unit:μ m	σ_x	σ_y	σ_x	σ_y	σ_x	σ_y	x	y
Case 1	5.17	5.2	9.11	9.48	11.5	9.5	2.22	1.83
Case 2	5.02	5.2	7.71	9.01	9.58	9.01	1.91	1.73
Case 3	4.75	4.95	7.06	8.6	7.92	8.53	1.75	1.74
Case 4	8.16	8.34	10.3	9.56	12.7	9.53	1.56	1.14
Case 5	11.2	11.3	15.1	12.1	14.5	12.1	1.29	1.07
Case 6	25.2	25.1	37.2	22.9	35	22.9	1.39	0.91

Table 5: Standard Deviation Beam Size at the Main IP

Standard deviation beam size	CSR/ISR off, w/o dp/p		CSR/ISR off, with dp/p		CSR/ISR on, with dp/p		Relative growth of rms beam size	
unit: μ m	σ_x	σ_y	σ_x	σ_y	σ_x	σ_y	x	y
Case 1	5.57	5.29	22.83	20.14	23.70	20.24	4.26	3.82
Case 2	5.17	5.80	15.13	12.99	15.97	12.96	3.09	2.23
Case 3	4.86	4.85	10.65	19.98	11.09	19.98	2.78	10.94
Case 4	8.33	8.31	11.78	20.20	14.11	20.29	1.69	2.44
Case 5	11.20	11.28	20.08	12.59	19.30	12.59	1.72	1.12
Case 6	25.19	25.07	41.95	24.01	39.26	23.96	1.56	0.96

DISCUSSION

Without energy spread and SR effects, the Gaussian fit beam sizes and standard deviation beam sizes are close to design values.

Cases 1, 2, and 3 have the same design β* of 0.018/0.18 m at IP. The IP Gaussian beam size with energy errors decreases as β functions in FF and chicane decrease from case 1 to case 3. The tail distribution decreases from case 1 to case 3 too, except the vertical tail in case 3.

Cases 4, 5, 6 have similar optics functions in the chicane. The FF β functions decrease as the β* increases from 0.054/0.54 m to 0.1/1 m and 0.5/5 m, respectively. The growth of vertical beam size and tail is decreased as β* is increased.

This study shows that in terms of small core beam size at the IP, case 3 is the best lattice. However, the vertical tail in this case is large. An alternative is case 5, which is less sensitive to the chromatic and sextupole aberrations and where the relative tail growth is smaller.

REFERENCES

[1] M. Borland, APS Tech. Rep. LS-287 (2000).
[2] Grote and F.C. Iselin, CERN/SL/90-13(AP)(Rev. 5).